



Magnetic and Structural Behaviour of Cobalt & Nickel Substituted Calcium W-Type Nanosize Hexaferrites

SMITA C TOLANI^{1*} and KISHORCHANDRA G. REWATKAR²

¹St. Vincent Pallotti College of Engineering and Technology, Nagpur, India.

²Dr. Ambedkar College, Nagpur, India

Abstract

The available literature and research work on W-type hexaferrites is mainly focused on Co- and Ni-based calcium W-type hexagonal ferrites with a variety of cationic substitutions. The Modifications in the properties of the Calcium W-type ferrite based on Ni²⁺ as the divalent metal ion, however, is not studied sufficiently in the research literature available. In this study, the focus is mainly on the effects of substitution of Ni²⁺ on the properties of CaCo₂W Hexaferrites. The investigations carried out are mainly XRD, SEM and VSM. The main objective of this research investigation is to study the effect of substitution of Nickel and Cobalt on the structural and magnetic properties of calcium W-type hexaferrite CaCo_{2-2x}Ni_xFe₁₆O₂₇ (x=0, 1 and 2). XRD analysis and characterization revealed slight decrease in the values of lattice constants 'a' and 'c' with increase in concentration 'x'. The particle size was confirmed from SEM and TEM images. The analysis of VSM for magnetic properties reveals decrease in coercivity and increase in the values of saturation magnetization as concentration increases. The results of measurements made by the various experimental techniques and the observations were compared to understand the crystalline and magnetic structure of the compounds.



Article History

Received: 04 August 2021

Accepted: 22 October 2021

Keywords

Ca-Hexaferrites;
Co₂W Hexaferrite;
c-axis Anisotropy;
Ni-Substitution;
Sol-Gel Auto
Combustion
W-type Ferrite;
VSM.

Introduction

Magnetic materials are ubiquitous throughout industry. Two well-known major branches of magnetic materials are metallic magnetic materials and ceramic mag-oxides. These magnetic materials are called ferrites. There are three types of ferrite materials: spinels, garnets and hexaferrites.¹⁻⁵ The spinels and garnets exist as cubic crystal structures,

whereas the hexaferrites exist as hexagonal crystal structures. Basically, different crystal structures will give them different magnetic, dielectric and mechanical properties.⁶ They possess some common properties like high values of permeability & permittivity, low magnetic losses, high Curie temperature, good mechanical strength, and high values of magnetisation. W type hexaferrite crystal

CONTACT Smita C Tolani ✉ smitatolani@gmail.com 📍 St. Vincent Pallotti College of Engineering and Technology, Nagpur, India.



© 2021 The Author(s). Published by Enviro Research Publishers.

This is an Open Access article licensed under a Creative Commons license: Attribution 4.0 International (CC-BY).

Doi: <http://dx.doi.org/10.13005/msri/180305>

structures belong to P63/mmc space group, and they have a stacking sequence of RSSR*S*S*, which is very similar to the stacking sequences of M type hexaferrites. Barium W-type ferrites has a molecular formula of $\text{BaMe}_2\text{Fe}_{16}\text{O}_{27}$, where Me is usually divalent transition metal ions which occupies tetrahedral, octahedral and trigonal bipyramidal sites. Most of the divalent metal substituted W-type hexaferrites (i.e. Zn_2W , Ni_2W and Fe_2W) hexaferrites have magnetic anisotropy perpendicular to the c-axis; however Co_2W hexaferrites have c-axis anisotropy.⁷

In Calcium W-type hexagonal structure it is reported that the Fe ions have seven different sites namely 4fvi, 2d, 12k, 6g, 4f, 4fiv, and 4e or there exists five magnetic sites.⁸ The substitution of different divalent and trivalent ions into the lattice of Calcium W-type hexagonal ferrites can improve the magnetic characteristics and properties like permeability, and saturation magnetization.⁹ Hexaferrites are the materials having a hexagonal crystal structure. There are basically six different types of hexagonal ferrite structures like: W, M, Z, Y, U and X. The general formula of hexagonal ferrites can be depicted as $\text{MxMez}(\text{Fe}_2\text{O}_3)_y$, where the ratios of x/y for W, M, Z, Y, U and X are found to be 1:8, 1:6, 1:4, 1:3, 2:9 and 1:7 respectively.¹⁰⁻¹² Like Z type hexaferrites, the preferred magnetization of W type hexaferrites varies with different metal substitution.¹³⁻¹⁴

The divalent and trivalent cations when added to the sub lattices of W-type hexagonal ferrite have been found to create various applications. Hexagonal ferrites synthesized incorporating many methods of preparation and different physio-chemical conditions exhibits the complexities of structure and properties of these nanocrystals.¹⁵ W-type Barium Hexaferrite with cobalt and Nickel substitution in the earlier known studies exhibits slight change in lattice constants 'a' and 'c' with addition of nickel in prepared barium cobalt hexaferrite powder.¹⁶ $\text{BaNi}_2\text{Fe}_{16}\text{O}_{27}$ hexaferrite is known to exhibit soft ferrite nature, while other nickel substitutes barium cobalt ferrites show hard ferrite behavior.¹⁶ In the current work, the samples of W-type Cobalt and Nickel substituted calcium hexaferrite have been synthesized by microwave induced sol-gel auto combustion method. The effects of Co^{2+} and Ni^{2+} ions on magnetic and structural properties of calcium W-type hexaferrites have been investigated.

Synthesis

Microwave induced sol-gel auto combustion method is a simple and cost effective way to synthesize nano-scale ferrite material powders. The sol-gel auto combustion synthesis method involved the preparation of sol by dissolving stoichiometric amount of A.R. grade calcium nitrate, iron nitrate, cobalt nitrate, nickel nitrate and urea in deionised water. The solution was then heated at 80°C on a magnetic hot plate with continuous stirring till a thick gel is formed. After evaporation of water the solution became a thick brown colored gel. The gel was then fired inside the microwave oven. The metal nitrates mixed with urea decomposed to give flammable gases such as NH_3 , O_2 , and NO respectively. After the point of spontaneous combustion, the solution became a solid which burns at temperatures above 1200°C. The combustion process yields the material is porous, easily crumbled with voids and loose due to gases escaping during the combustion reaction.¹⁶ The powder is then grinded into fine powder using a pestle and mortar. The Microwave induced sol-gel auto combustion technique is a quick process producing very fine nanohexaferrite particles. The synthesized ferrites were put in a Muffle furnace in the crucible and they were sintered at the temperature of 800°C for the duration of 4 hours by gradually increasing the temperature of the furnace at the rate of 100°C every hour. After sintering the furnace was cooled at the same slow rate. Then the material powdered samples were further grinded for 4 hours duration to fine particles in a mortar and pestle.

Results and Discussions

X-Ray Diffraction

The XRD pattern of sample $\text{CaCo}_{2-x}\text{Ni}_x\text{Fe}_{16}\text{O}_{27}$ for concentrations $x = 0, 1, 2$, were sintered at the temperature of 800°C as shown in Fig. 1-3. The X-ray diffraction patterns shown in Figures 1-3 were used to determine the structural properties of the synthesized Calcium W-type Hexagonal Ferrite materials. All diffraction patterns correspond to a hexagonal crystal lattice and structure as published in ICDD-#78-0135 and they belong to space group P63/mmc. The XRD analysis reveals presence of W-ferrites (JCPDS No. 780135).

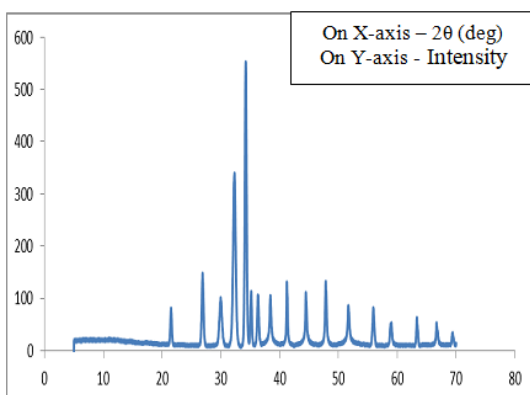


Fig.1: XRD pattern of $\text{CaCo}_{2-x}\text{Ni}_x\text{Fe}_{16}\text{O}_{27}$ for $x=0$

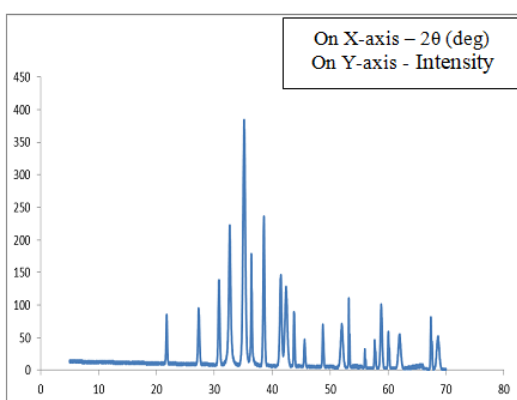


Fig.2: XRD pattern of $\text{CaCo}_{2-x}\text{Ni}_x\text{Fe}_{16}\text{O}_{27}$ for $x=1$

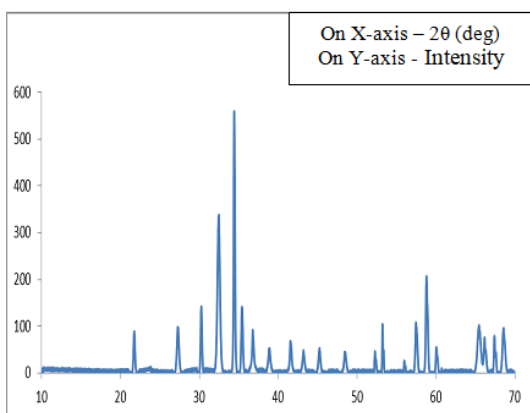


Fig.3: XRD pattern of $\text{CaCo}_{2-x}\text{Ni}_x\text{Fe}_{16}\text{O}_{27}$ for $x=2$

The cell volume and lattice parameters of the W phases are as tabulated in Table 1. The lattice constants 'a' and 'c' for Co_2W are found to be slightly lower than those for Ni_2W .²² The cell volume 'V' of Co_2W is observed to be slightly lower than that

of Ni_2W . This is not the result of differences in the ionic radii of Ni^{2+} and Co^{2+} ions, as Co^{2+} ions have a slightly higher ionic radius at octahedral site (0.88 Å) than Ni^{2+} (0.83 Å).

The values of the observed X-ray density (ρ_x) were found to increase with the value of x, as shown in Table 1. The enhancement in the density of X-rays is due to the enhancement in the molecular weight of Calcium W-type hexagonal ferrite when Co^{2+} cations completely replaces Ni^{2+} cations in the crystal lattice.¹⁸⁻¹⁹

Table 1: XRD Calculations for $\text{CaCo}_{2-x}\text{Ni}_x\text{Fe}_{16}\text{O}_{27}$

Concen- -tration	Lattice constant a(Å)	c(Å)	V=a ² c (Å) ³	Porosity D (%)	D (nm)
x=0	5.9608	32.8732	1167.6	46	23.19
x=1	5.7893	32.8021	1095.79	44	27.68
x=2	5.7023	32.7210	1062.42	43	48.94

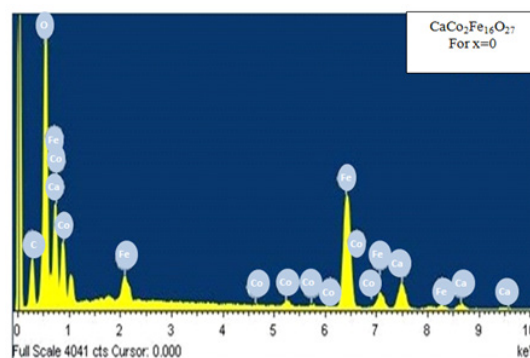


Fig. 4: EDX Spectrum of $\text{CaCo}_2\text{Fe}_{16}\text{O}_{27}$ for $x=0$

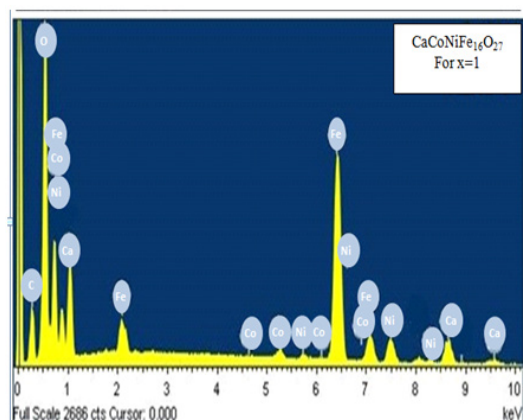


Fig. 5: EDX Spectrum of $\text{CaCoNiFe}_{16}\text{O}_{27}$ for $x=1$

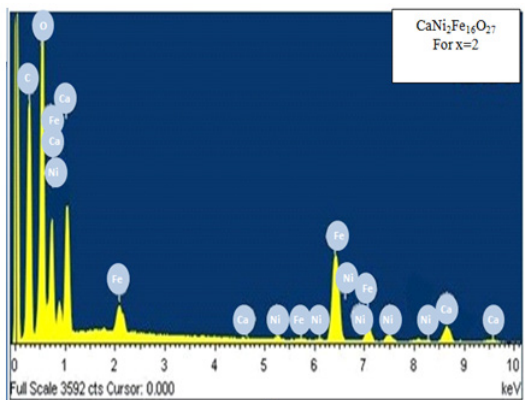


Fig. 6: EDX Spectrum of $\text{CaCo}_2\text{Fe}_{16}\text{O}_{27}$ for $x=2$

Energy Dispersive X-ray Spectroscopy (EDX)

Figures. 4, 5 and 6 shows the EDX Spectra of $\text{CaCo}_{2-x}\text{Ni}_x\text{Fe}_{16}\text{O}_{27}$ for $x=0, 1$ and 2 respectively giving the evidence for the presence of cobalt, nickel, oxygen, calcium and iron in the stoichiometric proportion as desired in the composition of the samples prepared.

Morphology

Figure. 7 shows SEM images of $\text{CaCo}_{2-x}\text{Ni}_x\text{Fe}_{16}\text{O}_{27}$ for $x = 1$ sintered at the temperature of 800°C . This representative SEM image reveals granular hexagonal structure mainly composed of regular hexagonal plates having wide distribution of particle size. These hexagonal plates have diameters ranging between 30-50 nm with average grain size of the order of 40 nm. Ca-W hexagonal ferrite has single-domain size of nearly 30 nm,²⁰ hence we can say that the sample consists of particle in multi-domain. The porosity of these particles exhibit relatively low porosity.

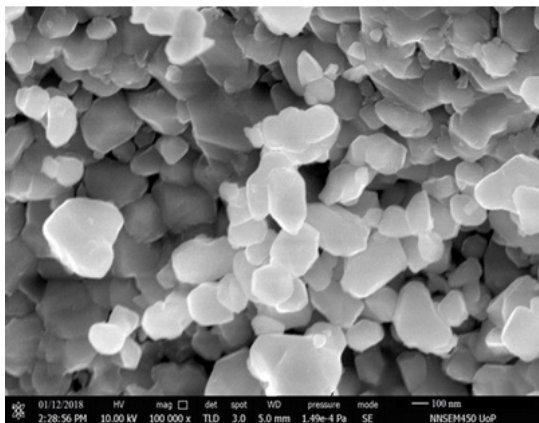


Fig. 7: SEM micrograph of $\text{CaCoNiFe}_{16}\text{O}_{27}$

Transmission electron microscopy (TEM) images of all samples are shown in Figure.8 giving an idea about the particle size and size distribution of Ni and Co substituted Ca-W hexaferrite. The average size of the nanoparticles in the samples were calculated to be 48nm, 47nm and 46 nm for $\text{CaCoFe}_{16}\text{O}_{27}$, $\text{CaCoNiFe}_{16}\text{O}_{27}$ and $\text{CaNi}_2\text{Fe}_{16}\text{O}_{27}$ respectively. These TEM micrographs were taken by TEM-CM200 operating at the voltage of 20-200KeV.

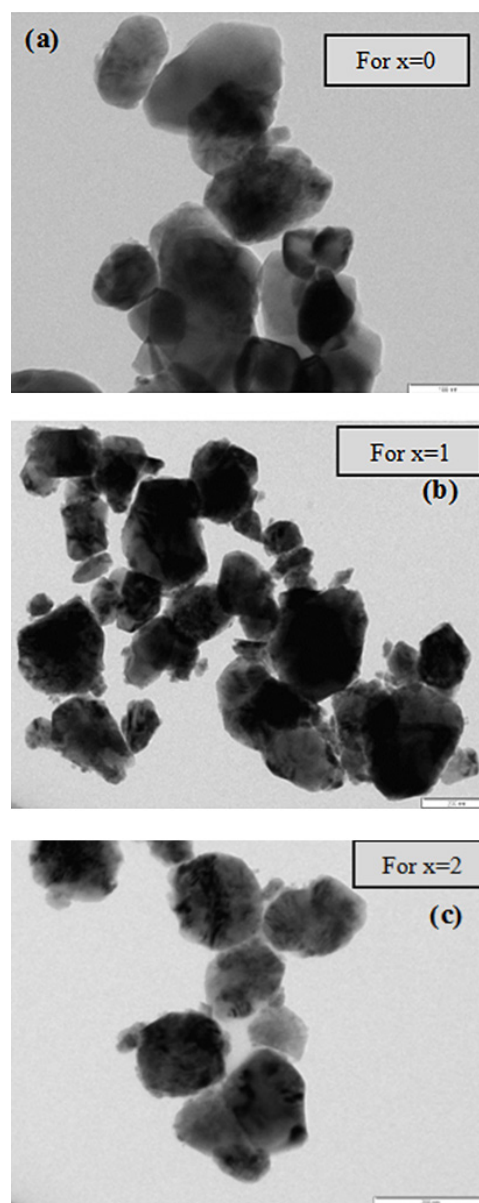


Fig. 8: TEM images of $\text{CaCo}_{2-x}\text{Ni}_x\text{Fe}_{16}\text{O}_{27}$ for (a) $x=0$, (b) $x=1$ and (c) $x=2$

Magnetic Behavior

The Hexagonal ferrite structure consists of closely packed oxygen in the lattice with the cations existing at the octahedral, trigonal bipyramidal and the tetrahedral sites. The ion hopping mechanism between tetrahedral and octahedral sites has a small probability than that for octahedral–octahedral sites. The hopping of ions between tetrahedral–tetrahedral sites does not exist which facilitates the Fe^{+3} ions occupying the tetrahedral sites. If any Fe^{+2} ions are developed during the sintering process, then they occupy octahedral sites.²¹

Ca-hexaferrites with Ni^{2+} substitutions show higher saturation magnetization values than that of unsubstituted samples analyzed in this research. Figures 9 & 10 show hysteresis curves of samples at $x=0$ and $x=1$ respectively. The increase of the saturation magnetization from 1.12 emu/g for Co_2W to 1.20 emu/g for Ni-W is due to the substitution of Ni^{2+}

ions by Co^{2+} ions at spin-up sites.^{21,22} The coercivity decreased from 1137 Oe down to 784 Oe as shown in Table 2. This may be correlated with the increase of particle size of the Ca-W phase. The decrease in the coercivity of the sample sintered at 800°C is correlated with phase transformation from hard Ca-W to soft Ca-W Phase with enhanced particle size. This decrease is due to the enhancement of the particle size beyond the critical single domain size as reflected in the SEM image.

Table 2: VSM Data Calculations for $\text{Ca}_2\text{Co}_{2-x}\text{Ni}_x\text{Fe}_{16}\text{O}_{27}$

Concentration	Ms (emu/g)	Mr (emu/g)	Hc (Oe)
$x=0$	1.12	0.548	1137
$x=1$	1.20	0.484	784

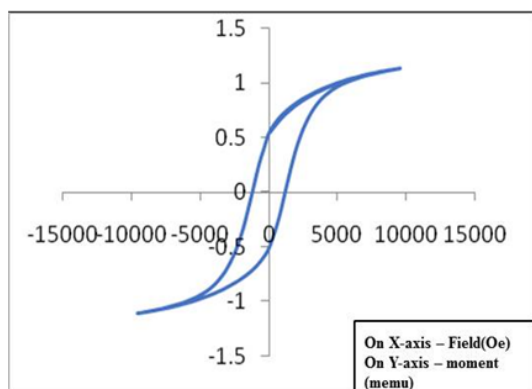


Fig. 9: B-H curve for $\text{Ca}_2\text{Co}_2\text{Fe}_{16}\text{O}_{27}$

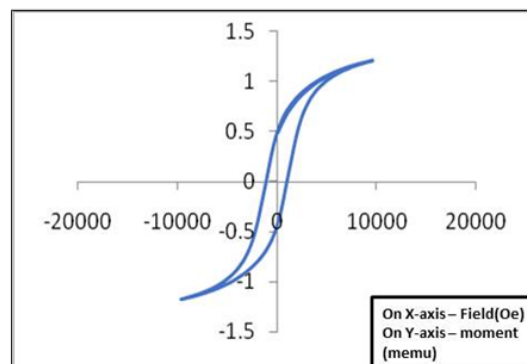


Fig. 10: B-H curve for $\text{Ca}_2\text{CoNiFe}_{16}\text{O}_{27}$

Conclusion

With microwave induced sol-gel auto combustion route, Ni and Co substituted calcium W-type hexagonal ferrite nano-particles have been effectively synthesized. The XRD data exhibits the presence of single phase W-type hexagonal ferrite. There is a single magnetoplumbite phase as no extra lines were reported in the samples. The indexed space group for the samples seen is found to be SG: P63/mmc (No. 194). The lattice unit cell dimensions 'a' and 'c' for Co_2W ferrite synthesized are found to be slightly less as compared to those for Ni_2W . The doping concentrations of Ni and Co are at appropriate stoichiometric ratio depicted in the

EDX result. These elements are combined together to form the hexagonal phase of the ferrite material which was confirmed by XRD study.

SEM micrograph shows that the particles have hexagonal-plate structure. The SEM micrograph of the nickel and cobalt doped samples show a consistent grain growth and the samples appear to be mixture of homogenous individual particles. TEM images show that the sample has nanocrystalline nature. The saturation magnetization (Ms) increases with the substitution of Ni ions in the calcium nano-hexaferrite. The enhancement in the Ms is due to the spin up state replacement

of Fe³⁺ ions. The value of coercivity (H_c) is found to decrease with Ni substitution due to variation in structure and anisotropy field. The increase in the value of coercivity of hexaferrite can be attributed to the particle size and domain structure.

Acknowledgement

The author Smita Chandar Tolani thank the Head of the Research Laboratory , Dr. Ambedkar College, Nagpur for providing the necessary help in synthesis and characterisation of the materials along with discussions while writing this paper. The author acknowledges the facilities provided by SAIF, Kochi for the measurements and characterisations namely XRD, SEM, and VSM of the samples.

Funding

- No financial sources or help was taken during this research.
- This research did not receive any specific grant from funding agencies in the public, commercial , or not-for-profit sectors.

Conflict of interests

- The authors declare that they have no known competing financial interests or personal relationships that could have appeared to influence the work reported in this paper.
- The author declare no conflict of interest.

References

1. B. Lax, K. J. Button, *Microwave Ferrites and Ferrimagnetics* (McGraw-Hill Book Company, Inc., 1962). Goldman, "Modern Ferrite Technology, 2nd Ed.", Springer, 2006.
2. G.F. Dionne, "Magnetic Oxides", Springer, 2009.
3. U. Ozgur, Y. Alivov, H. Morkoc, "Microwave ferrites, part 1: fundamental properties", *J Mater Sci: Mater Electron* (2009) 20:789–834.
4. R. C. Pullar, "Hexagonal ferrites: A review of the synthesis, properties and applications of hexaferrite ceramics", *Progress in Materials Science* 57 (2012) 1191–1334.
5. V. G. Harris, "Modern Microwave Ferrites", *IEEE Trans. Magn.* 48, 1075 (2012).
6. Santhosh Kumar M. V. , G.J. Shankarmurthy, E. Melagiriappa , Ashok Rao & K. K. Nagaraja, *Journal of Superconductivity and Novel Magnetism*, 33, pages2821–2827 (2020).
7. T. M. Perekalina, M. A. Vinnik, R. I. Zvereva, and A. D. Shchurova, "Magnetic properties of hexagonal ferrites with weak exchange coupling between sublattices," *Sov. J. Exp. Theor. Phys.*, vol. 32, p. 813, 1971.
8. P.S.Sawadh, D.K.Kulkarni, *Mater.Chem. Phys.*63(2000)170.
9. L.X.Wang,J.Song,Q.T.Zhanga,X.J.Huang,N.C.Xua, *J.AlloysCompd.*481(2009)863.
10. V. G. Harris, A. Geiler, Y. Chen, S. Yoon, M. Wu, A. Yang, Z. Chen et al., "Recent advances in processing and applications of microwave ferrites", *J. Magn. Magn. Mater.* 321, 2035 (2009).
11. J. Smit and H. P. J. Wijn, *Ferrites*. New York: Wiley, 1959, pp. 204–206.
12. R. Sagayaraja, T. Dhineshkumarb, A. Prakashb, S. Aravazhib, G. Chandrasekarand, D. Jayarajanc, S. Sebastiana, *Chemical Physics Letters* 759 (2020) 137944.
13. K. Haneda, A.H. Morrish, *Phase Transitions* 24 (1990) 661.
14. X. Wang, D. Li, L. Lu, X. Wang, *J Alloys Compd.* 273 (1996) 45.
15. Chetna C.Chauhan, Rajshree B. Jotania, *Nanosystems: Physics, Chemistry, Mathematics*, 2016, 7 (4), P. 595–5.
16. Gawali. S. R, Moharkar. P. R, Rewatkar. K. G, Nanoti. V. M., *J. of BionanoFrontier Special Issue* 5 (2012), 26-32
17. L. Rezlescu, E. Rezlescu, P. Popa, N. Rezlescu, Fine barium hexaferrite powder prepared by the crystallisation of glass, *Journal of Magnetism and Magnetic Materials*, 193 (1999) 288-290.
18. A. Awadallah, S.H. Mahmood, Y. Maswadeh, I. Bsoul, M. Awawdeh, Q.I. Mohaidat, H. Juwhari, Structural, magnetic, and Mossbauer spectroscopy of Cu substituted M-type hexaferrites, *Materials Research Bulletin*, 74 (2016) 192-201.
19. Gawali. S. R, Moharkar. P. R, Rewatkar. K. G,

- Nanoti. V. M., *J. of Bionano Fontier Special Issue 5* (2012), 26-32.
20. D. Hemeda, A. Al-Sharif, O. Hemeda, Effect of Co substitution on the structural and magnetic properties of Zn-W hexaferrite, *Journal of magnetism and magnetic materials*, 315 (2007) L1-L7.
21. Muhammad JavedIqbal and FarohaLiaqut, *J. Am. Ceram. Soc.*, 93[2] (2010), 474-480.
22. A. Collomb, P. Wolfers, X. Obradors, Neutron diffraction studies of some hexagonal ferrites: BaFe₁₂O₁₉, BaMg₂-W and BaCo₂-W, *Journal of magnetism and magnetic materials*, 62 (1986) 57-67.